Supporting Information

Design and Evaluation of a Thiazoline-Appended Imidazole based Fluorescent Turn ON Chemosensor for Hg^{2+} ion Detection: Spectroscopic Characterization and Solid State Film Applications

Bharathkumar Thangaraj [a] Suresh Ranganathan, [b,c] Ravichandran Cingaram,[a] Lakshmipriya Kannan,[a] Sathiyanarayanan Kulathu Iyer,[d] Karthikeyan Natesan Sundaramurthy,[a*]

[a] Department of Chemistry, Easwari Engineering College, India

[b] Department of Chemistry, Karpagam Academy of Higher Education, India.

[c] Centre for Material Chemistry, Karpagam Academy of Higher Education, India.

[d] Chemistry Division, School of Advanced Sciences, Vellore Institute of Technology (VIT), India.

Table of Contents

Fig.S1. and Fig. S2 are NMR details of **2TA**……………….............................. Page No: 02

Fig.S3. and Fig. S4 are NMR details of probe **BTA**………............................... Page No: 03

Fig.S5. and Fig. S6 are FT-IR and HR-MS spectra of probe **BTA** ………..…........ Page No: 04

Fig S7. UV-vis and fluorescence spectra of BTA towards anions........................... Page No: 05

Fig S8. Photographs of fluorescence enhancement of BTA-Hg^{2+} solution............. Page No: 05

Fig. S9. Anti-interference study of **BTA** towards other ions…………..…....…… Page No: 06

Fig. S10. Job's plot for **BTA** Vs Hg^{2+} ……………………………..…..…....…… Page No: 06

Fig. S11. HR-MS spectrum of **BTA**-Hg^{2+} complex ………...……………..…..… Page No: 07

Fig. S12. Nonlinear least-square fitting plot of **BTA** and Hg^{2+}…...…………..…..… Page No: 07

Fig. S13. FT-IR spectrum of probe **BTA** and **BTA**-Hg^{2+} ………………………….…….. Page No: 08

Fig. S14. pH studies of **BTA** and **BTA**-Hg^{2+} ……………………...……..…….. Page No: 08

Fig S15. Emission and life time spectra of **BTA**/PVA towards increasing Hg^{2+}..…Page No: 08

Table S1. Comparison of Hg^{2+} sensing performance with reported probes.…….. Page No: 10

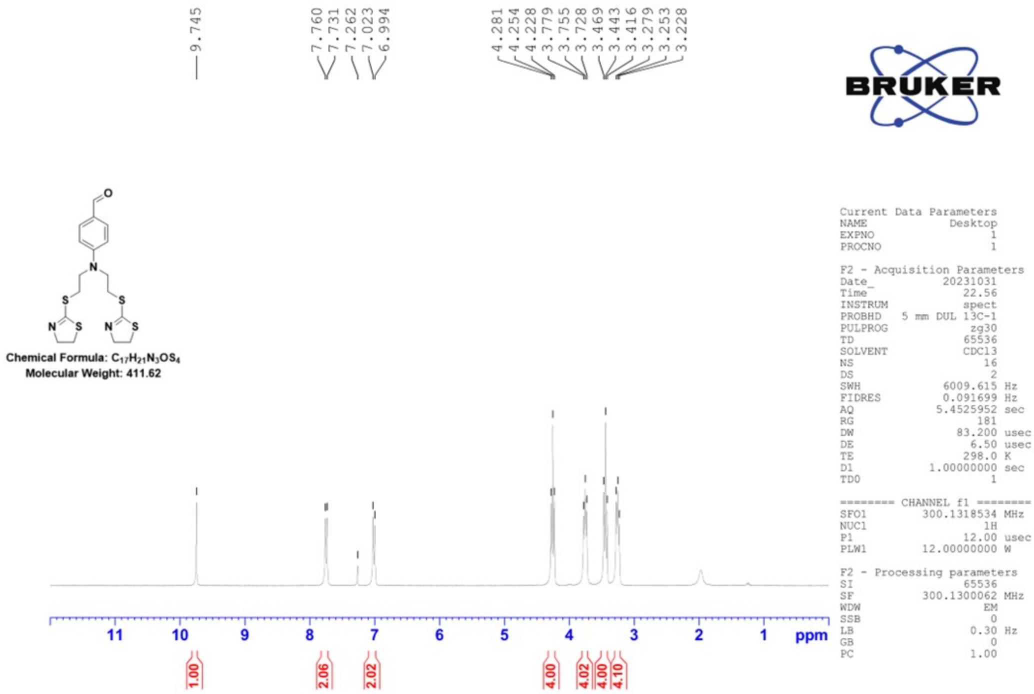

Figure S1. ^1H NMR spectra of **2TA** in $CDCl_3$

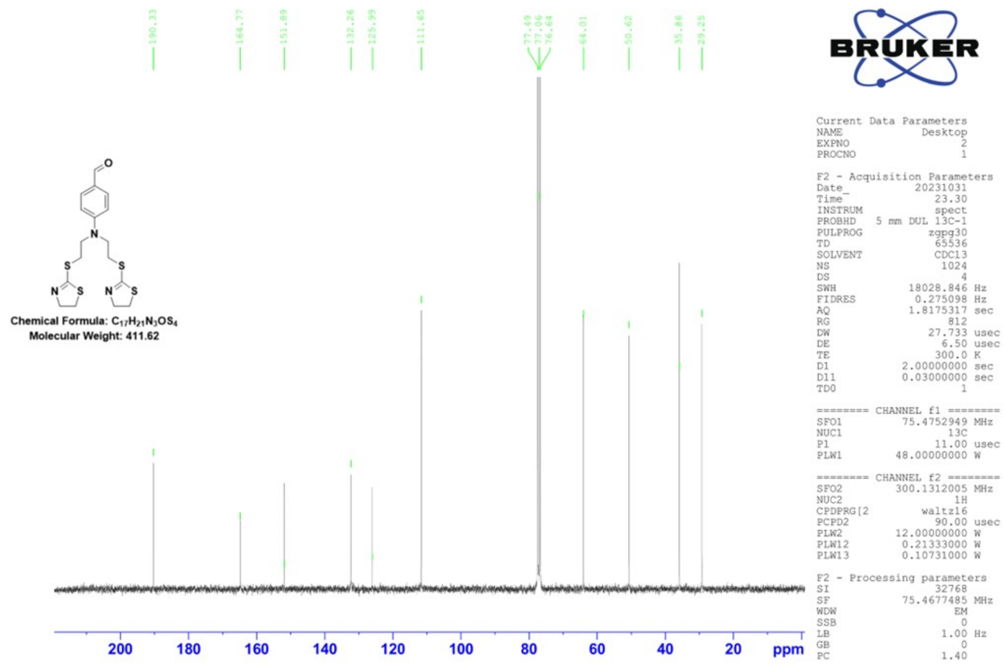

Figure S2. ^{13}C NMR spectra of **2TA** in $CDCl_3$

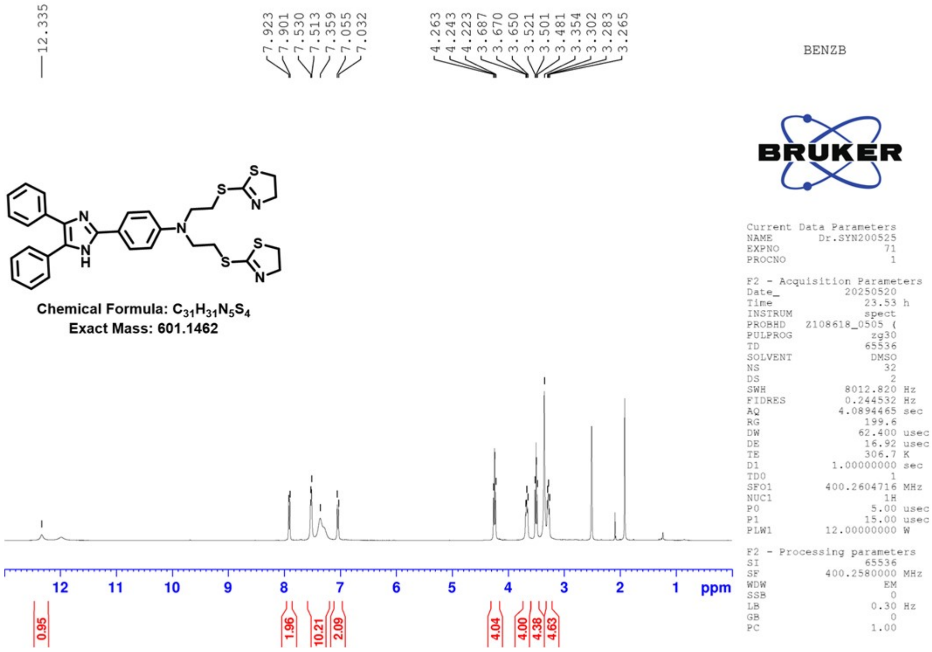

Figure S3. ^{1}H NMR spectra of probe **BTA** in DMSO-d_6

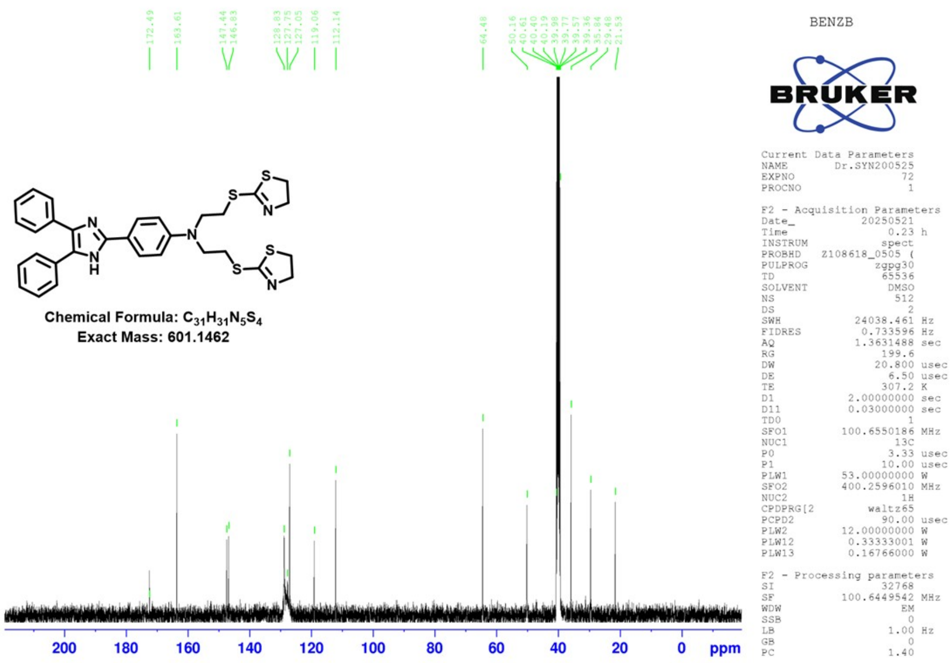

Figure S4. ^{13}C NMR spectra of probe

BTA in DMSO-d_6

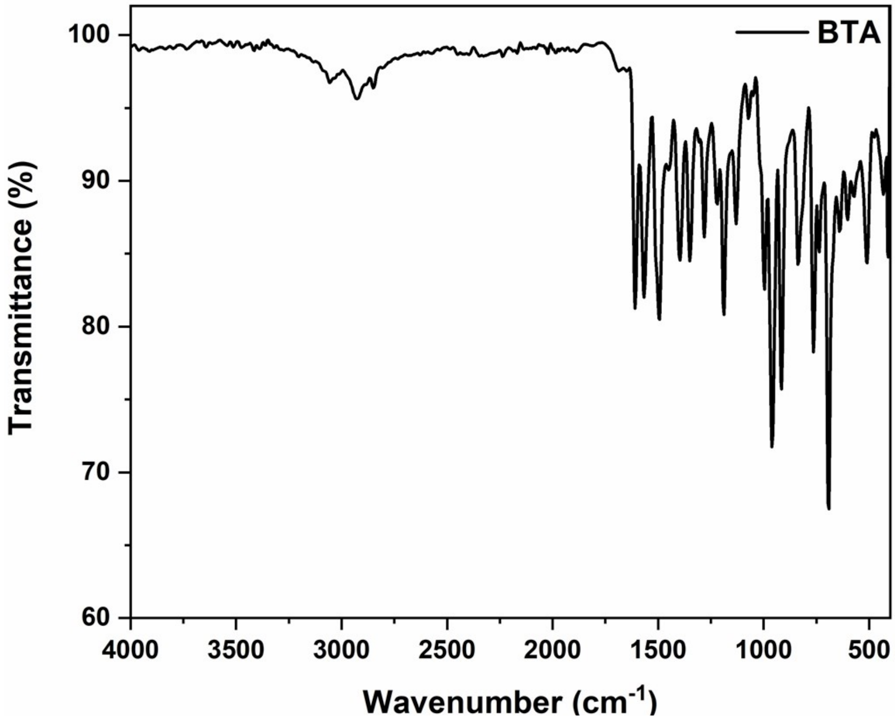

Figure S5. FT-IR spectra of probe **BTA**

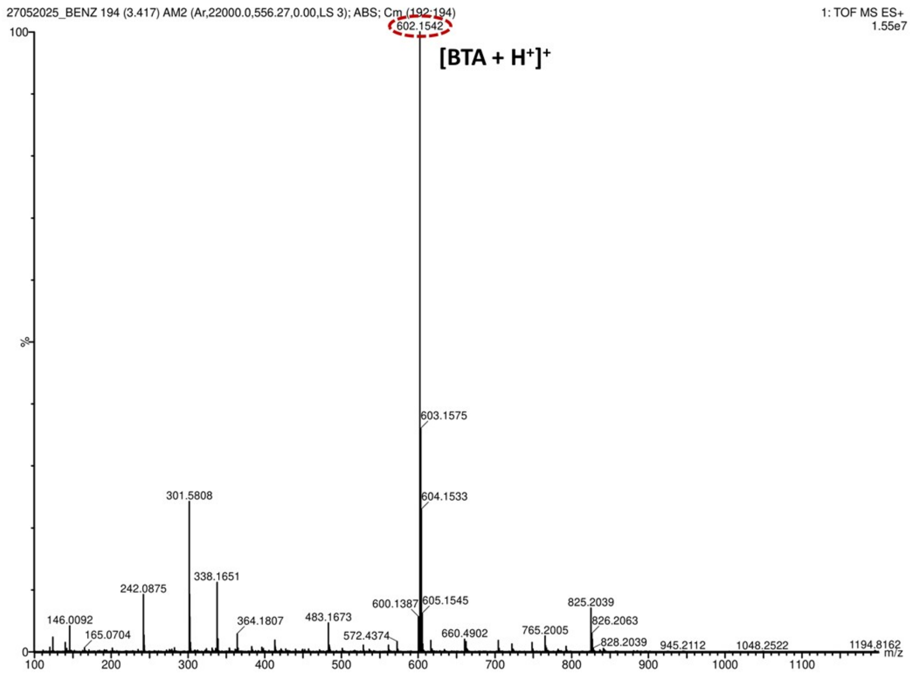

Figure S6. HR-MS spectrum of probe **BTA**.

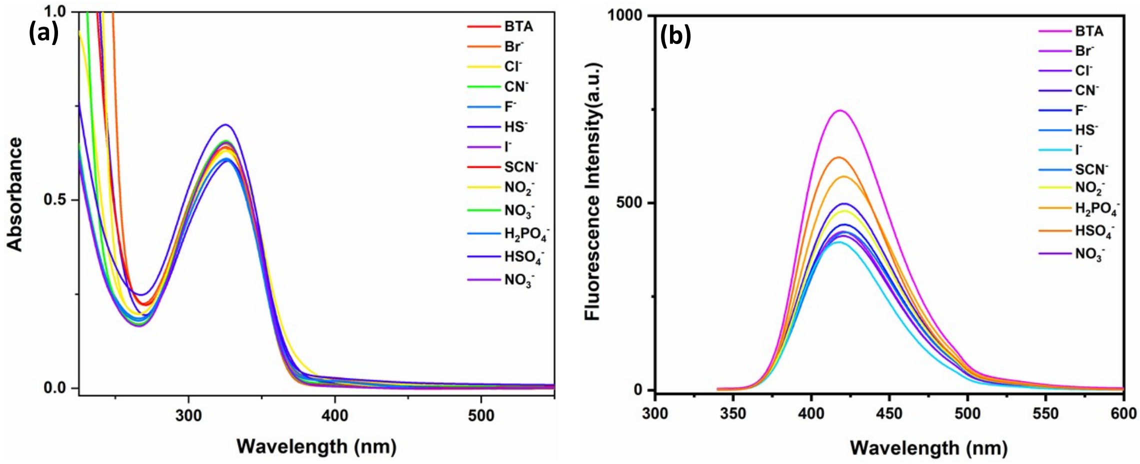

Figure S7. (a) UV-vis absorption and (b) fluorescence spectra of probe **BTA** (20 μM) in (CH_3CN: H_2O) (6:4, v\v) solution in response to 1 mM of diverse anions (5 equiv.).

Figure S8. Photographs displaying fluorescence enhancement upon increasing concentration of analyte to **BTA** solution.

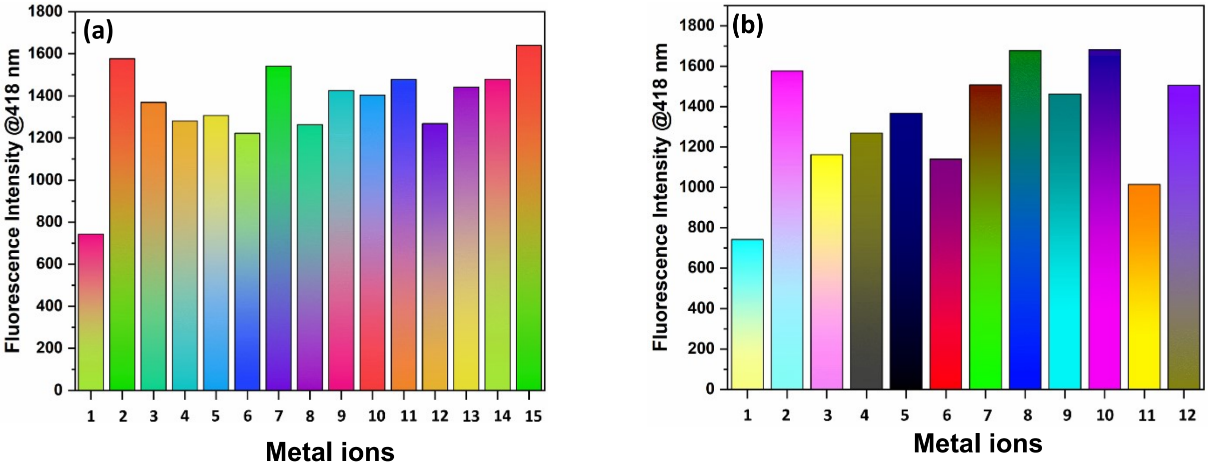

Figure S9. Fluorescence response of **BTA** in a mixture of (CH_3CN: H_2O) (6:4, vv) to **(a)** coexisting ions: (1) BTA; (2) BTA-Hg^{2+}; (3) BTA-Hg^{2+} + Cu^{2+}, Fe^{3+}; (4) BTA-Hg^{2+} + Na+, Fe^{2+}; (5) BTA-Hg^{2+} + Ca^{2+}, Cu^{2+}, (6) BTA-Hg^{2+} + K+, Zn^{2+}; (7) BTA-Hg^{2+} + Ni^{2+}, Cr^{3+}; (8) BTA-Hg^{2+} + Cr^{6+}, Zn^{2+}; (9) BTA-Hg^{2+} + Co^{3+}, Ba^{2+}; (10) BTA-Hg^{2+} + Zn^{2+}, Cu^{2+};(11) BTA-Hg^{2+} + Pb^{2+}, Mg^{2+};(12) BTA-Hg^{2+} + K+, Mg^{2+};(13) BTA-Hg^{2+} + Cd^{2+}, Zn^{2+};(14) BTA-Hg^{2+} + Li+, Al^{3+}; (15) BTA-Hg^{2+} + Mg^{2+}, Mn^{2+}. **(b)** mixed ions (1) BTA; (2) BTA-Hg^{2+}; (3) BTA-Hg^{2+} + Ni^{2+}, Cl^-; (4) BTA-Hg^{2+} + Ba^{2+}, $H_2PO_4^-$; (5) BTA-Hg^{2+} + Ca^{2+}, Br-; (6) BTA-Hg^{2+} + Pb^{2+}, CN^-; (7) BTA-Hg^{2+} + Cr^{3+}, NO_3^-; (8) BTA-Hg^{2+} + Cu^{2+}, HSO_4^-;(9) BTA-Hg^{2+} + Zn^{2+}, I^-; (10) BTA-Hg^{2+} + Cd^{2+}, F^-; (11) BTA-Hg^{2+} + Li^+, HS^-; (12) BTA-Hg^{2+} + Mg^{2+}, SCN^-.

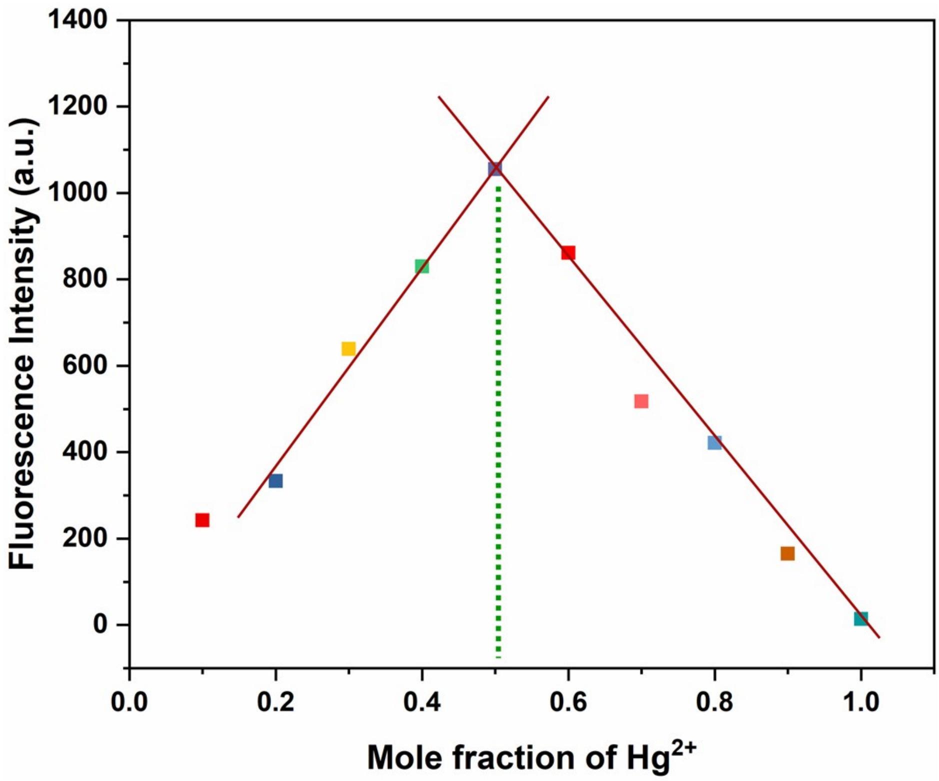

Figure S10. Job's plot for probe **BTA** Vs Hg^{2+}

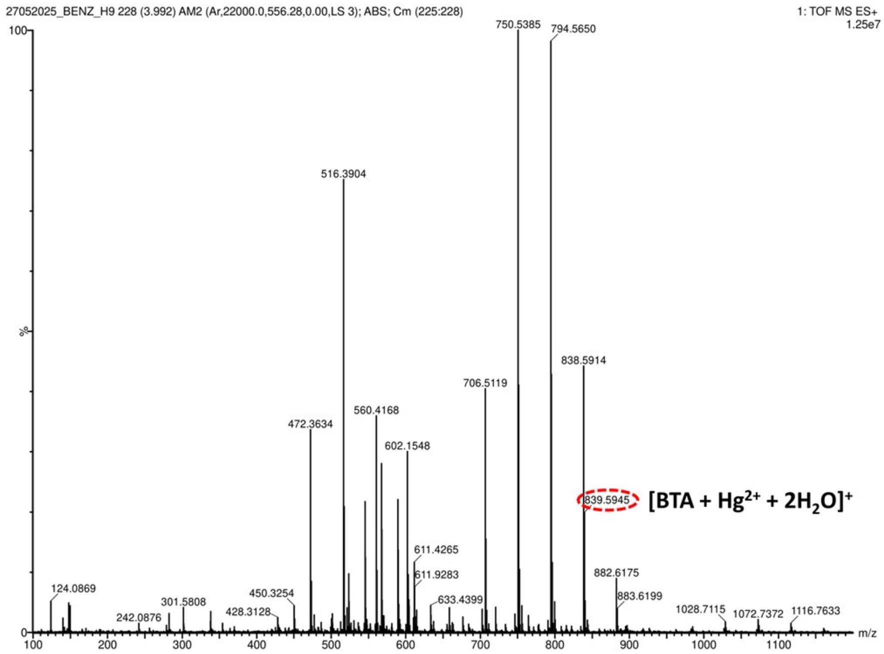

Figure S11. HRMS spectra of **BTA-**Hg^{2+} complex.

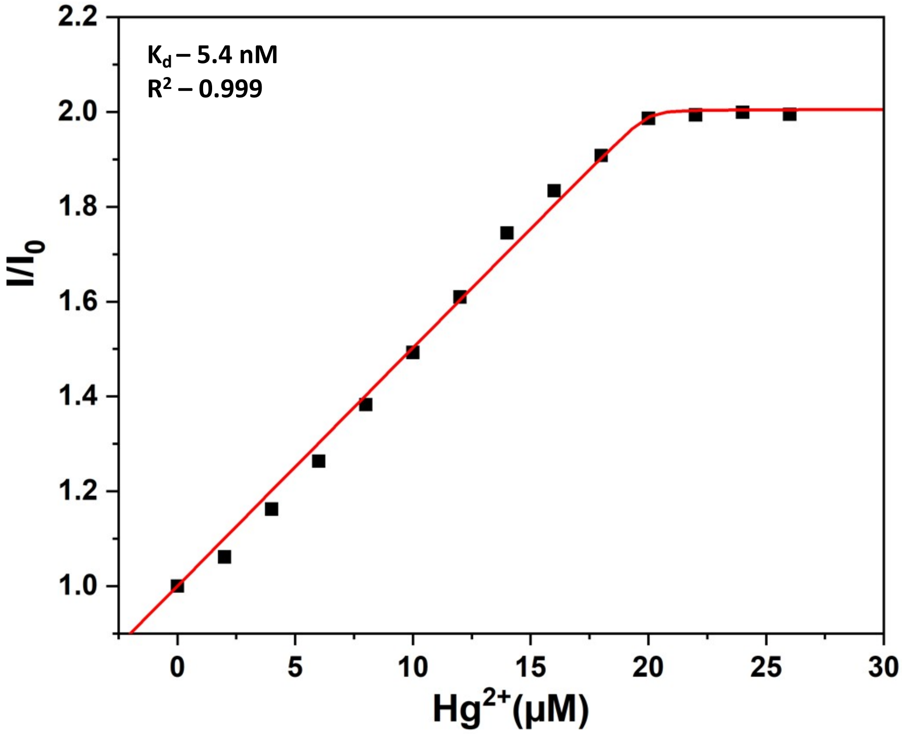

Figure S12. Nonlinear least-square fitting of the fluorescent emission intensity changes of BTA vs concentration of Hg^{2+} in aqueous acetonitrile medium using 1:1 complex binding equation.

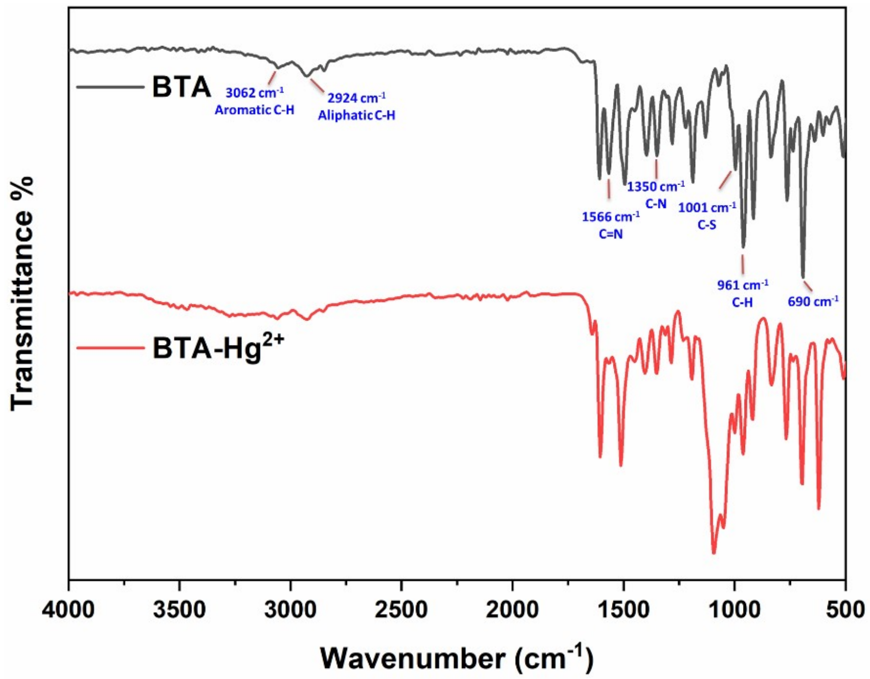

Figure S13. FT-IR spectra of **BTA** and **BTA**-Hg^{2+} complex.

S1. pH Studies

To assess the physiological application, the pH dependence of the chemoprobe BTA in CH_3CN/H_2O (6:4, v/v) was examined using fluorescence spectroscopy. As shown in Fig. S13, under acidic conditions (pH 2-4), the probe (BTA) and metal complex (BTA-Hg^{2+}) shows high fluorescence due to protonation of the imidazole group. As pH increases above 4, fluorescence intensity of BTA decreases sharply and attains its normal state, in contrast, the BTA-Hg^{2+} system maintains strong fluorescence over pH 4-10, indicating stable complex formation. At higher pH (11-12), a slight decrease in fluorescence is observed, likely due to increased basicity. Overall, the probe performs optimally in the pH range 4-10, making it suitable for Hg^{2+} detection under environmental and biological conditions.

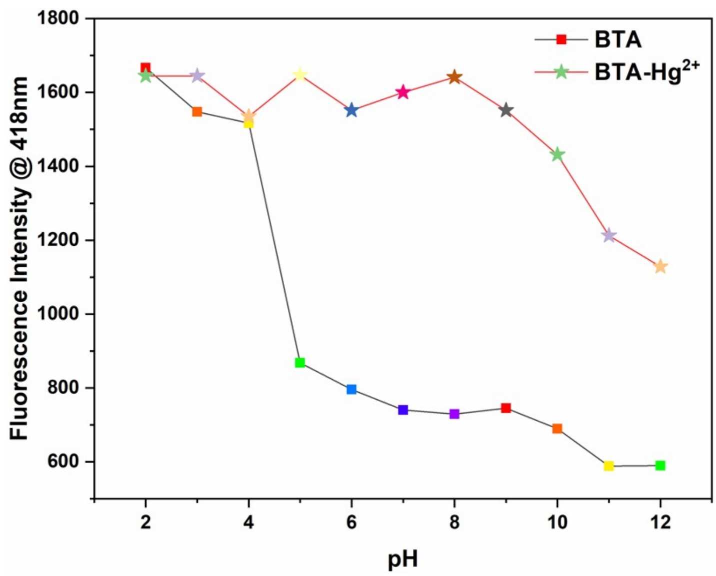

Figure S14. Effects of pH on the emission intensity of probe **BTA** (20 μM) in the absence and presence of Hg^{2+} in CH_3CN/H_2O (6:4, v/v).

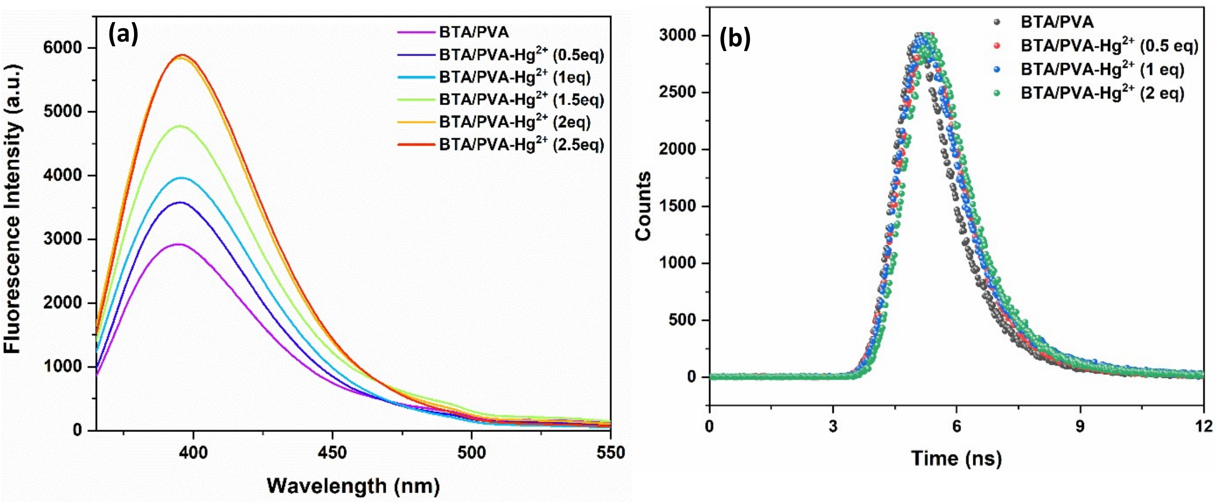

Figure S15. (a) Fluorescence response (b) life time spectra of BTA/PVA towards increasing concentration of Hg^{2+}.

Table S1. Comparison of Hg^{2+} sensing performance with reported probes

Ref No	Chemoprobe	Detection limit	Detection method	Interference studies	Reversibile studies	Response time	Solid state detection of Hg^{2+}
1	Rhodamine Phenolphthalein	334 nM	Fluorescence ON	Done	Done	12 mins	Filter paper
2	Dansyl	509 nM	Fluorescence OFF	-	Done	-	-
8	Thiourea	0.5 µM	Fluorescence ON	-	-	-	-
4	Piperazine benzimidazole	0.68 µM	Fluorescence OFF	Done	Done	-	-
5	Thiourea	4.92 µM	Fluorescence ON	Done	-	-	-
6	Chitosan-BODIPY	1.51 µM	Fluorescence OFF	Done	-	-	-
7	BODIPY	0.05 µM	Fluorescence OFF	Done	-	-	-
8	Coumarin	3.78 µM	Colorimetric	Done	Done	-	-
9	Dihydropyrimidine	0.5 µM	Quenching	-	-	-	-
	BTA (This work)	**114 nM**	**Fluorescence ON**	**Done**	**Done**	**4 sec**	**PVA film**

Reference

1 A.S. Hussein, F. Lafzi, S. Bayindir, H. Kilic and M. Toprak, *ChemPlusChem*, 2024, **89**, e202300649.

2 I. Lourenço, F. Duarte, G.M. Dobrikov, A. Kurutos, I. Slavchev, J.L. Capelo-Martínez, H.M. Santos and C. Lodeiro, *J. Mater. Chem. C*, 2025, **13**, 6708-6719.

3 P. Mohanty, P.P. Dash, S. Naik, R. Behura, M. Mishra, H. Sahoo, S.K. Sahoo, A.K. Barick and B.R. Jali, *J. Photochem. Photobiol. A*, 2023, **437**, 114491.

4 L. Wang, C. Lou, S. Duan, D. Cheng, A. Wang, B. Zhao, H. Zhao, G. Yin and M. Zhao, *Inorg. Chem. Commun.*, 2020, **119**, 108096.

5 H. Kim, M. Lee, J.J. Lee, E.K. Min, K.T. Kim and C. Kim, *J. Photochem. Photobiol. A*, 2022, **428**, 113882.

6 D. Wang, L. Marin and X. Cheng, *Int. J. Biol. Macromol.*, 2022, **198**, 194-203.

7 C. Chan, H. Liu and Z. Xue, *Microchem. J.*, 2021, **166**, 106247.

8 S. Schoeman, N. Mama and L. Myburgh, *New J. Chem.*, 2025, **49**, 1745-1754.

9 S. Saha, J. De, R. Choudhury, S.J. Chaudhuri, H. Banik, S.A. Hussain and T.K. Misra, *Inorg. Chim. Acta*, 2025, **577**, 122480.